Comparison of Tripole and Vector Antenna Applications for Radio Astronomy

H. Timurcan Evci
University of Twente, Telecommunication Engineering Group
P.O. Box 217, 7500 AE, Enschede, The Netherlands
Email: h.t.evci@student.utwente.nl

***Abstract*—Frequencies below 30 MHz are the least discovered range in the radio astronomy spectrum, due to the ionospheric and man-made interferences. This frequency band can give information about the formation of the first structures in the universe, and many other discoveries in the cosmos. Due to the ionospheric cutoff frequency of about 10 MHz and distortion, ground based arrays cannot observe below this cutoff frequency, therefore a space mission is required. The only space mission to observe the low frequency range, RAE-B, had low angular resolution and sensitivity as it was a single antenna measurement instrument.**

Recent studies are focusing on improving the angular resolution and sensitivity by proposing alternative sensor arrays and imaging algorithm designs. Knapp et al. proposed to improve the sensitivity by using a vector antenna to measure all of the six electromagnetic field signals in a single measurement. The claim is that the vector antenna has a 3 dB advantage in SINR compared to the more commonly used tripole antenna. The tripole antenna is able to measure the complete electric field, meaning that the magnetic field can be calculated with Maxwell's equations. Knapp et al. assumed that the rank of the total electromagnetic field vector is 6 and, the measured electric and magnetic field signals are uncorrelated for the vector antenna. However, the electric and magnetic fields are coupled with Maxwell's equations, meaning that the field signals are correlated.

In this research, the performances of the tripole and vector antennas are compared by mathematically working out the steering vectors and SINR and simulating them, to see whether the claim of Knapp et al. is valid. Also, to introduce both antennas, their models, S-parameter plots and radiation patterns are simulated in the HFSS software. The mathematical foundations showed that the assumptions of Knapp et al. are incorrect. MATLAB simulations confirmed the calculations, as for uncorrelated and correlated signal and noise conditions, the SINR did not change, meaning that the claim is invalid.

***Index Terms*—Tripole Antenna, Vector Antenna, Radio Astronomy, HFSS, SINR.**

I. Introduction

In radio astronomy, the high frequency band (1-30 MHz) is considered as the least discovered range in the EM spectrum. This particular frequency range is important, as it can provide information about the formation of the cosmos. By measuring the electric and magnetic fields of radiation in this frequency range, the formation of the first stars and galaxies, and other astrophysical processes can be revealed. Due to ionospheric interferences, ground based antenna arrays are not able to access the HF part of the spectrum. Added to the ionospheric interferences, man-made interferences in this frequency range make it very challenging to identify EM waves of cosmic sources. In order to avoid interferences and distortions from the ionosphere as much as possible, a space mission is required. The Radio Astronomy Explorer B [1] is the only space mission that observed and mapped the frequency range of 25 kHz to 13.1 MHz, however with a low angular resolution of 60 degrees. Recent studies are focusing on improving the angular resolution by proposing alternative sensor and imaging algorithm designs. For aperture synthesis, the complexity on a single spacecraft and system complexity in different nodes is a trade-off factor to consider. Knapp et al. [2] proposed to increase the complexity of each node by using a vector antenna to measure all of the six electromagnetic field signals. The claim is that the vector antenna has a 3 dB advantage in SINR compared to the more commonly used crossed dipole or tripole antenna. The main research question of this paper is, whether this claim is true.

To investigate the validity of the SINR claim, the tripole and vector antennas have to be analysed. This paper is split into three parts. In the first part, the tripole antenna and vector antenna will be introduced and their performances will be simulated. The HFSS (High Frequency Structural Simulator) software is used to design both antennas and to simulate the radiation patterns, S-parameter plots and field magnitude plots. In the second part, the assumptions and claims made by Knapp et al. will be investigated. In order to check whether the assumptions and claims are true, the steering vectors and SINR performances of both sensors will be studied by providing mathematical foundations. In the third part, the findings will be simulated and the results of both sensors will be compared and discussed. This paper will be concluded by reflecting on the mathematical foundations and simulations to see if the claim of Knapp et al. is true, and finally recommendations for the future will be addressed.

II. Electromagnetic Field Sensors

A. Tripole Antenna

The tripole antenna consists of three orthogonal and equal length electric dipoles, each located at one of the three directions of the 3D space. The length of each dipole is half a wavelength. The main advantage of this antenna is that it is able to measure the complete electric field vector. By Maxwell's 3rd and 4th equations, the electric and magnetic

fields are related. This means that the whole electromagnetic field can be measured by using a tripole antenna.

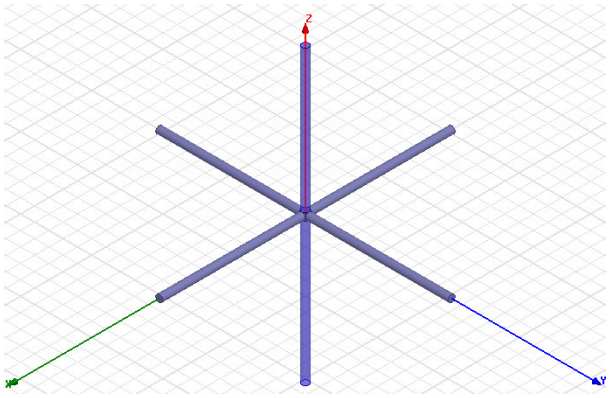

Fig. 1: Tripole Antenna HFSS Model

The tripole antenna HFSS model is depicted in Fig. 1. For a frequency of 10 MHz, the wavelength is 30 m, meaning that the length of each dipole should be 15 m. Due to the fact the simulations were slow and erroneous for 15 m, the antenna lengths have been downscaled to 1 m. The dipoles are fed with equal and positive currents with no phase difference. The resulting simulated radiation pattern of the tripole can be seen in Fig. 2.

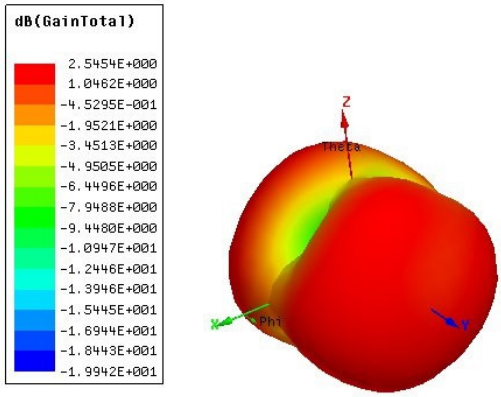

Fig. 2: Tripole Antenna Radiation Pattern

Eriksson [3] modelled the radiation pattern by calculating the Poynting vector and plotted them for different current amplitudes and phases. Comparing the simulated radiation pattern to Fig. 3.1 of [3], they differ significantly. The simulated pattern was expected to be doughnut shaped, however, due to the low gain in certain directions, the radiation pattern is not a full doughnut. By simulating the S-parameters, the reason becomes apparent. Fig. 3 shows that only the excitation in the x direction is radiating at 275 MHz, however, the excitations in the y and z directions aren't radiating.

The feeding points of each dipole are lumped port excitations and are centered in between the dipoles. One reason that the simulated pattern is not as expected, could be the fact that these excitations are in physical contact with each other and are affecting the current distributions of the dipoles. In essence, the tripole antenna can be understood by studying Eriksson's tripole model and observing the radiation patterns for different current distributions.

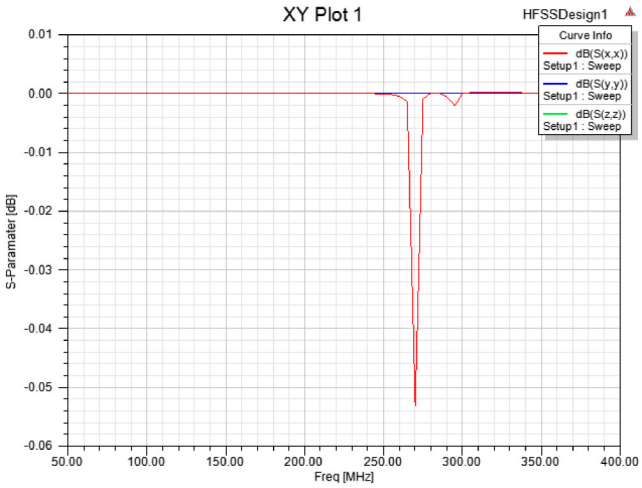

Fig. 3: Tripole Antenna S-Parameter

B. *Vector Antenna*

The vector antenna consists of three orthogonal dipole antennas and three orthogonal magnetic loop antennas, which is depicted in Fig. 4. As aforementioned, three orthogonal dipole antennas form the tripole antenna, which measures the complete electric field. Meanwhile, three orthogonal magnetic

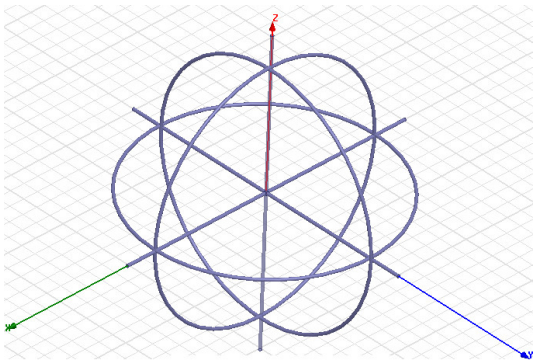

Fig. 4: Vector Antenna HFSS Model

loop antennas form an antenna called the magnetic loop triad, which measures the complete magnetic field. The advantage of the combination of the tripole antenna and the magnetic loop triad is that it can measure the complete electromagnetic field in a single measurement. Knapp et al. used the sum and difference hybrid to serve as a dipole and loop antenna at the same time. This power divider hybrid is connected to two ports of a loop with a circumference of 0.1λ (the same as a magnetic loop).

The sum and difference hybrid that was chosen to be simulated is the magic tee junction [4]. The magic tee waveguide has 4 ports; one sum port (or H-plane port), one difference port (or E-plane port) and two collinear ports. The difference port is located on the upper face of the magic tee on the +z

axis, while the sum port is located on the outer face on the +x axis.

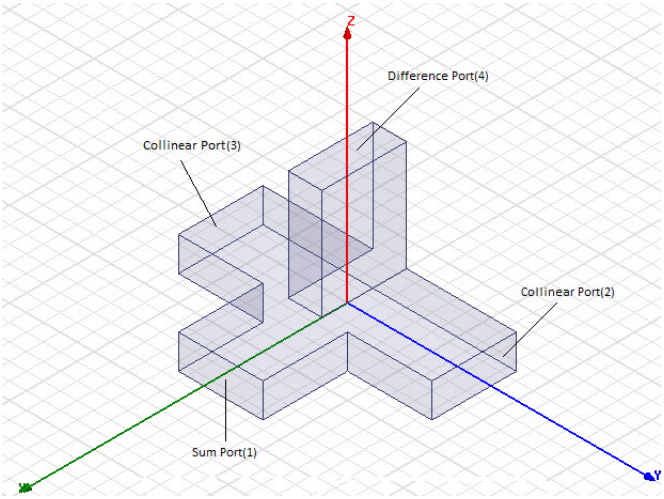

Fig. 5: Magic Tee HFSS model

When two inputs are fed into the collinear ports, the output at the H-plane port will be the sum of both inputs, while the output at the E-plane port will be the difference of the inputs. Respectively, the E-plane port serves as a dipole and the H-plane port serves as a loop, when fed from the two collinear inputs. If the input is fed into the E-plane port, the input is divided equally on the collinear outputs with a phase difference of 180 degrees.

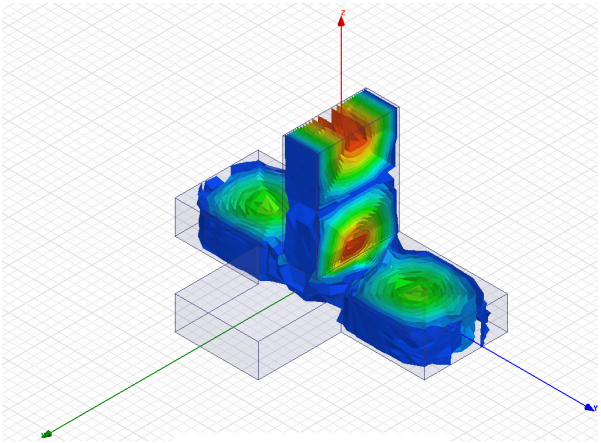

Fig. 6: E-Field Plot, input fed from E-plane port

The HFSS model of the magic tee is depicted in Fig. 5. The length, width and height of the boxes have been taken from the HFSS user guide [5]. The size parameters on the guide are for microwave devices at a frequency of 4 GHz. The dimensions of rectangular waveguides are available in the Chapter 3.3 of [4] and are scalable with wavelength. By scaling the parameters given in the user guide by a factor of 100, a frequency of 40 MHz is achieved. A box has been created with a length of 5.0 m, a width of 5.0 m and a height of 2.0 m. The box is duplicated around the necessary axes and then united to form the magic tee.

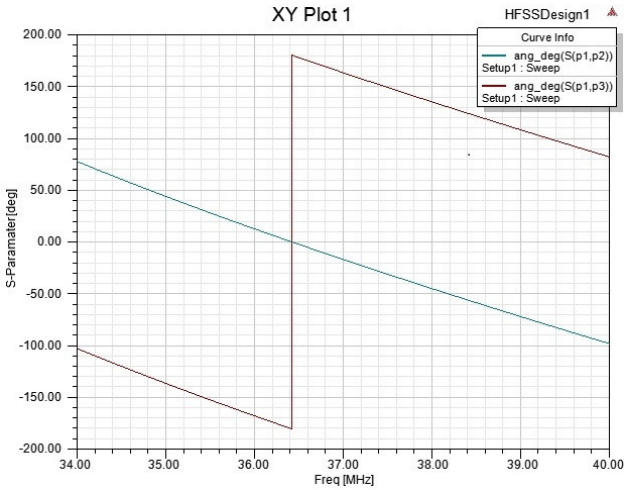

Fig. 7: Phase Plot of S12 and S13

To demonstrate that the waveguide is operating, the electric field has been plotted for an input fed into the E-plane port on Fig. 6. The input has been divided equally for the collinear ports as expected, however the phase difference is not visible. Therefore, the phase of the S-parameters is plotted. The phases of the S12 and S13 parameters are depicted in Fig. 7. Port 1, Port 2 and Port 3 represent the E-plane port and the two collinear ports respectively. There is a 180 degree phase difference between the collinear ports as expected. This plot also shows that the magic tee is operating at around 36.5 MHz.

Due to the fact that the magic tee is designed for microwave devices, the dimensions of the model designed for low frequencies become considerably large. Therefore, using a traditional vector antenna or another sum and difference hybrid would be more reasonable.

III. Comparison of Sensors

In this section, the tripole and vector sensors will be compared. The comparisons will be made according with the assumptions and claims Knapp et al. make. The main claim is that the vector antenna has a 3 dB advantage in SINR compared to the tripole antenna. The assumptions made by Knapp et al. to arrive at this claim will be investigated in the following subsections. Throughout [2], there are two critical assumptions that stand out:

A1: *The rank of the vector space of the total field is 6*
The complete three-dimensional electromagnetic field of a point p can be represented as,

$$F(p) = \begin{bmatrix} E_x(p) \\ E_y(p) \\ E_z(p) \\ H_x(p) \\ H_y(p) \\ H_z(p) \end{bmatrix} \tag{1}$$

while the total field, $\mathbf{F}_T$, is the superposition of the fields of each point. According to the authors of [2], the rank of $\mathbf{F}_T$ is 6 without proof for the vector antenna, meaning

that the electromagnetic field covariance matrix has rank 6. The covariance matrix described in Eq. 3 of [2] is the matrix multiplication of the steering vector and its hermitian. Comparing the steering vectors of both the vector antenna and the tripole antenna is essential, in the sense of investigating the validity of the assumption. If the steering vector of the tripole antenna is the same as the steering vector of the vector antenna, the assumption of the total field having rank 6 is incorrect.

A2: *The electric and magnetic field signals are uncorrelated for the vector antenna*
The second assumption Knapp et al. makes is that the electric and magnetic field measurements for the vector antenna are independent. The tripole antenna inside the vector antenna measures the complete electric field and the magnetic loop triad measures the complete magnetic field. The tripole antenna by itself is capable of measuring the complete electromagnetic field, as the magnetic field can be calculated electric field with the help of Maxwell's equations. As both antennas are capable of measuring the complete electric field, the main element that should affect the SINR is the magnetic field vector. According to Knapp et al., the measured magnetic field signal of the vector antenna should have better SINR compared to the calculated magnetic field signal of the tripole antenna. Therefore, by combining assumption **A1** and **A2**, the steering vectors and the SINR of both sensors will be compared, in order to see if the claim of the vector antenna performing better than a tripole antenna is valid.

A. Steering Vector Comparison

Maxwell's equations, more specifically, Faraday's and Ampere's laws represent the relationship between the electric and magnetic fields. The tripole antenna measures the complete electric field, meaning that by Maxwell's equations the magnetic field can be calculated, while the vector antenna measures the complete electric and magnetic field without any calculations. The steering vectors of the tripole antenna and the vector antenna will be investigated.
Wong [6] describes the electromagnetic field vector at a single point, in terms of angular coordinates and polarization as,

$$\begin{bmatrix} e_p \\ h_p \end{bmatrix} = \begin{bmatrix} e_x(\theta_p, \phi_p, \gamma_p, \eta_p) \\ e_y(\theta_p, \phi_p, \gamma_p, \eta_p) \\ e_z(\theta_p, \gamma_p, \eta_p) \\ h_x(\theta_p, \phi_p, \gamma_p, \eta_p) \\ h_y(\theta_p, \phi_p, \gamma_p, \eta_p) \\ h_z(\theta_p, \gamma_p) \end{bmatrix} \tag{2}$$

where θ, ϕ, γ and η denote the elevation angle, azimuth angle, auxiliary polarization angle and polarization phase difference respectively. He defines the steering vector of the vector antenna as,

$$s_{vector} = \begin{bmatrix} cos\phi_p\ cos\theta_p & -sin\phi_p \\ sin\phi_p\ cos\theta_p & cos\phi_p \\ -sin\theta_p & 0 \\ -sin\phi_p & -cos\phi_p\ cos\theta_p \\ cos\phi_p & -sin\phi_p\ cos\theta_p \\ 0 & sin\theta_p \end{bmatrix} \begin{bmatrix} sin\gamma_p e^{j\eta_p} \\ cos\gamma_p \end{bmatrix} \tag{3}$$

By splitting e_p and h_p, Wong assigns these vectors to the tripole antenna and loop triad respectively. The steering vector for the tripole antenna becomes,

$$s_{tripole} = \begin{bmatrix} -sin\phi_p\ cos\gamma_p + cos\theta_p\ cos\phi_p\ sin\gamma_p e^{j\eta_p} \\ cos\phi_p\ cos\gamma_p + cos\theta_p\ sin\phi_p\ sin\gamma_p e^{j\eta_p} \\ -sin\theta_p\ sin\gamma_p e^{j\eta_p} \end{bmatrix} \tag{4}$$

Li [7] defines the electric field components in a right-handed polar coordinate system, e_ϕ, e_θ, $-e_r$. As the electric field produces a polarization ellipse, there is no field in the e_r direction, which means that the electric field becomes,

$$\mathbf{E} = E_\phi e_\phi + E_\theta e_\theta \tag{5}$$

From the polarization ellipse, the electric field components become apparent,

$$E_\phi = \mathbf{E} cos\gamma \tag{6}$$

$$E_\theta = \mathbf{E} sin\gamma e^{j\eta} \tag{7}$$

Using Maxwell's third equation, $\nabla \times \mathbf{E} = -\frac{\partial \mathbf{B}}{\partial t}$ for $\nabla = \left(\frac{\partial}{\partial r}, \frac{\partial}{\partial \phi}, \frac{\partial}{\partial \theta}\right)$, the magnetic field vector can be found using the curl representation in polar coordinates,

$$\nabla \times \mathbf{E} = \frac{1}{r^2 sin\theta} \begin{vmatrix} \mathbf{e_r} & r\mathbf{e}_\phi & rsin\theta \mathbf{e}_\theta \\ \frac{\partial}{\partial r} & \frac{\partial}{\partial \phi} & \frac{\partial}{\partial \theta} \\ E_r & rE_\phi & rsin\theta E_\theta \end{vmatrix} \tag{8}$$

Since there is no electric field in the e_r direction,

$$\nabla \times \mathbf{E} = \frac{1}{r^2 sin\theta} \begin{vmatrix} 0 & r\mathbf{e}_\phi & rsin\theta \mathbf{e}_\theta \\ \frac{\partial}{\partial r} & \frac{\partial}{\partial \phi} & \frac{\partial}{\partial \theta} \\ 0 & \mathbf{E} rcos\gamma & \mathbf{E} rsin\theta sin\gamma e^{j\eta} \end{vmatrix} \tag{9}$$

The curl of the electric field in polar coordinates becomes,

$$\nabla \times \mathbf{E} = -\frac{\mathbf{E} cos\gamma}{r}\ \mathbf{e}_\theta + \frac{\mathbf{E} sin\gamma e^{j\eta}}{r}\ \mathbf{e}_\phi \tag{10}$$

By converting the polar coordinates into cartesian coordinates and dropping the $\mathbf{E}$ and r terms (complete derivation available in Appendix A), the steering vector becomes a 6×1 vector,

$$s_{tripole} = \begin{bmatrix} -sin\phi_p\ cos\gamma_p + cos\theta_p\ cos\phi_p\ sin\gamma_p e^{j\eta_p} \\ cos\phi_p\ cos\gamma_p + cos\theta_p\ sin\phi_p\ sin\gamma_p e^{j\eta_p} \\ -sin\theta_p\ sin\gamma_p e^{j\eta_p} \\ -cos\theta_p cos\phi_p cos\gamma_p - sin\phi_p sin\gamma_p e^{j\eta_p} \\ -cos\theta_p sin\phi_p cos\gamma_p + cos\phi_p sin\gamma_p e^{j\eta_p} \\ sin\theta_p cos\gamma_p \end{bmatrix} \tag{11}$$

By comparing this vector to the steering vector in Eq.3, it is clear that the steering vectors of both antennas are equal as expected, meaning that assumption **A2** and consequently assumption **A1** is not correct.

B. Signal to Interference Plus Noise Ratio(SINR) Comparison

In this section, the signal to interference plus noise ratios(SINR) of the tripole antenna and vector antenna are compared. Knapp et al. claim that the vector antenna has a 3 dB advantage in sensitivity compared to the tripole antenna. They start by introducing the optimal SINR equation for adaptive processing,

$$SINR = \alpha \mathbf{s}^H \mathbf{R_n^{-1}} \tag{12}$$

where s is the steering vector and R_n is the noise covariance matrix. The noise covariance matrix for simplified noise plus interference is represented as,

$$R_n = \sigma \mathbf{I} + \beta \mathbf{d}\mathbf{d}^H \tag{13}$$

where d is the steering vector of an interfering source with intensity β. By setting $\mathbf{d}^H\mathbf{d} = 1$, the electric and magnetic components of d can be split up, as $\mathbf{d_e^H d_e} = \mathbf{d_h^H d_h} = 0.5$. However, to apply this operation, the measured electric and magnetic field signals must be uncorrelated. Assuming that all signals are uncorrelated and independent, Eq.11 of [2] is formed,

$$\eta = \frac{SINR_{vector}}{SINR_{tripole}} = 2\frac{\left(1 - \frac{\beta cos^2(\gamma)}{(\sigma+\beta)}\right)}{\left(1 - \frac{\beta cos^2(\gamma)}{(2\sigma+\beta)}\right)} \tag{14}$$

meaning that for $\beta = 0$, there is a factor 2 improvement in SINR. However, due to the fact that the electric and magnetic fields being heavily coupled by Maxwell's equations, the electric and magnetic field signals are correlated, therefore the SINR equations for both the tripole and vector antenna should be equal. To demonstrate that the SINR does not differ for the tripole antenna and the vector antenna, the SINR is investigated under correlated and uncorrelated signals in Section IV.

IV. Simulations

The SINR is simulated in MATLAB for correlated and uncorrelated electromagnetic signals. The tripole antenna has been simulated in such a way that it only measures the electric field signals and the magnetic field signals are stated as a correlation of the electric field signals. For 1000 sources, random field and noise vectors have been created. The noise vectors are created for a desired SINR of 30 dB. The electric field signals have been correlated to the magnetic field signals by a correlation factor of 0.9. The SINR has been simulated to be 30 dB for all combinations. The tripole antenna cannot measure the magnetic field directly, therefore the electric and magnetic field signals cannot be uncorrelated, therefore it is not simulated for the uncorrelated signal condition.

For the vector antenna, the assumption of Knapp et al. is that the signals are uncorrelated. Therefore, firstly, the simulations have been made for uncorrelated signals. Six uncorrelated random signal and noise vectors are simulated. The previous conditions for the tripole antenna (using 1000 sources and noise vectors for a desired SINR of 30 dB) have been repeated for the vector antenna. Again,the SINR has been simulated as 30 dB.

To prove that the assumption of Knapp et al. is incorrect, the vector antenna has been simulated by assuming that the signals are correlated. However, differing from the tripole antenna, the correlations can be investigated by two ways, as the tripole antenna element measures the complete electric field and the magnetic loop triad element measures the complete magnetic field, meaning that the magnetic field can be calculated from the electric field and vice versa. For both ways, the SINR's were simulated to be 30 dB.

The electric field measured by the tripole element and, the magnetic field measured by the loop element have the ability to give information to calculate their respective magnetic and electric fields, so the foundation of the claim that the vector antenna having improved SINR can be that the linear combination offers improved field signals. To investigate this, the linear combination of the measured and calculated fields, (i.e. correlated and uncorrelated fields) is created using the wave impedance equation,

$$Z_0 = \sqrt{\frac{\varepsilon_0}{\mu_0}} = \frac{|\,\mathbf{E}\,|}{|\,\mathbf{H}\,|} \tag{15}$$

where ε_0 is the vacuum permittivity and μ_0 is the vacuum permeability. The vectors $\mathbf{Z_1} = \mathbf{E} + \frac{\mathbf{E}}{Z_0}$ and $\mathbf{Z_2} = \mathbf{H} + Z_0\mathbf{H}$ are created to compare the SINR of the electric and magnetic field measurement SINR to the linear combination SINR. For both $\mathbf{Z_1}$ and $\mathbf{Z_2}$, the SINR has been calculated 30 dB.

The simulation is extended further by comparing the SINR for dependent and independent noise. First, the SINR is tested for independent noise for electric and magnetic field signals. Then, the SINR for the linear combination of the magnetic and electric field noise vectors is simulated. Again, using the wave impedance equation, Eq. 15, the dependent noise vector is created. The SINR did not differ for dependent and independent noise and is simulated to be 30 dB for both cases.

It is clear that the SINR doesn't change for tripole and vector antennas for different signal and noise conditions and are 30 dB for noise vectors with a desired SINR of 30 dB. Observing the mathematical foundations and simulation results, assumptions **A1** and **A2**, and consequently the claim of 3 dB advantage of SINR is not correct.

V. Conclusion and Future Work

This paper investigated the performance comparison of tripole and vector antennas. Tripole and vector antennas were modelled in HFSS and their radiation patterns and S-parameters have been simulated. Due to being inexperienced in HFSS, the radiation pattern of the tripole antenna is not as expected. However, by investigating the results of Eriksson **??**, the tripole antenna has been understood. The vector antenna simulations are as expected, however the dimensions of the magic tee are not feasible to implement in field testing. An alternative sum and difference hybrid or a traditional vector antenna would be more feasible to implement.

The assumptions of Knapp et al. have been investigated and, calculations and simulations showed that these assumptions are incorrect. Simulations for both antennas on SINR showed that the claim of having an advantage of 3 dB is not be true for uncorrelated and correlated signals, and even the

linear combination of these signals. Also, for dependent and independent noise vectors, the SINR did not change.

Field tests of Knapp et al. were in the initiation phase during the process of this research, therefore the claim of the 3 dB advantage is not verified yet. Due to the time constraint, the antennas were not tested on the field, which could have provided important information about the signal to interference plus noise ratio. Measuring fields in real life and comparing the results to the simulations would be the next step to verify whether the claim is correct or not.

APPENDIX A
DERIVATION OF THE STEERING VECTOR OF THE TRIPOLE ANTENNA

By continuing from Eq. 10 in section 3A, the magnetic field components of the steering vector can be derivated. First, the polar coordinates have to be converted to cartesian coordinates,

$$\begin{aligned} \mathbf{e_x} &= sin\theta_p cos\phi_p\ \mathbf{e_r} + cos\theta_p cos\phi_p\ \mathbf{e}_\theta - sin\phi_p\ \mathbf{e}_\phi \\ \mathbf{e_y} &= sin\theta_p sin\phi_p\ \mathbf{e_r} + cos\theta_p sin\phi_p\ \mathbf{e}_\theta + cos\phi_p\ \mathbf{e}_\phi \\ \mathbf{e_z} &= cos\theta_p\ \mathbf{e_r} - sin\theta_p\ \mathbf{e}_\theta \end{aligned} \tag{16}$$

Dropping the e_r terms,

$$\begin{aligned} \mathbf{e_x} &= cos\theta_p cos\phi_p\ \mathbf{e}_\theta - sin\phi_p\ \mathbf{e}_\phi \\ \mathbf{e_y} &= cos\theta_p sin\phi_p\ \mathbf{e}_\theta + cos\phi_p\ \mathbf{e}_\phi \\ \mathbf{e_z} &= -sin\theta_p\ \mathbf{e}_\theta \end{aligned} \tag{17}$$

Converting the polar coordinates to cartesian coordinates by filling them in the curl of electric field equation results in,

$$\begin{aligned} -\frac{\partial \mathbf{B_x}}{\partial t} &= -cos\theta_p cos\phi_p cos\gamma_p - sin\phi_p sin\gamma_p e^{j\eta_p} \\ -\frac{\partial \mathbf{B_y}}{\partial t} &= -cos\theta_p sin\phi_p cos\gamma_p + cos\phi_p sin\gamma_p e^{j\eta_p} \\ -\frac{\partial \mathbf{B_z}}{\partial t} &= sin\theta_p cos\gamma_p \end{aligned} \tag{18}$$

REFERENCES

[1] Alexander, J. K., Kaiser, M. L., Novaco, J. C., Grena, F. R., Weber, R. R., *"Scientific instrumentation of the Radio-Astronomy-Explorer-2 satellite"*, Astronomy and Astrophysics, vol. 40, no. 4, May 1975, p. 365-371.

[2] Knapp, M., Robey, F., Volz, R., Lind, F., Fenn, A., Seager, S., Morris, A., Silver, M., Klein, S., *"Vector Antenna and Maximum Likelihood Imaging for Radio Astronomy"*, 2016.

[3] Eriksson, S.,*"Study of tripole antenna arrays for space radio research"*, September 2003.

[4] Pozar, D. M., *"Microwave engineering"*,John Wiley & Sons, Inc. 2012.

[5] *"HFSS 10 User Guide"*, Ansoft Corporation, 2005.

[6] Wong, K. T., *"Direction finding / polarization estimation - Dipole and/or loop triad(s)"*, IEEETrans. Aerosp. Electron. Syst., vol. 37, pp. 679-684, Apr. 2001.

[7] Li, J., *"Direction and polarization estimation using arrays with small loops and short dipoles"*, IEEE Trans. Antennas Propagat., vol. 41, pp.379-387, Mar. 1993.